Geometric Morphometric Analysis of Sex Determination from Cranial Landmark Data Using Computed Tomography

Alexandra R. Klales[1], Niels Lynnerup[2], and Robert D. Hoppa[1]

[1] Department of Anthropology, University of Manitoba ● [2] Department of Forensic Medicine, University of Copenhagen

Introduction

Increasingly, computed tomography (CT) imaging has become an accepted and more utilized non-invasive method in skeletal biology. For sex estimation and classification, CT data have been used to generate 3D skeletal models (3DCT) from which morphological features of the skull have been assessed. Furthermore, 3DCT is one method that may be used in conjunction with discrete 3D coordinate data points, which are commonly employed for craniometric assessment of sex.

Several studies have assessed the precision of 3DCT acquisition of landmarks as compared to traditional caliper measurements and coordinate data collected by use of a digitizer on actual skulls, and no significant differences were found (Hildebolt *et al.* 1990; Williams & Richtsmeier 2003). Additionally, no significant differences were found in tests of observer error for landmark designation (Richtsmeier *et al.* 1995), suggesting that coordinate data from CT scans can be reliably used for sex estimation.

The purpose of this study was to assess the validity of craniometric landmark generation from 3DCT scans for sex determination. Both size and shape differences between the sexes were explored with 2D craniometrics and also with 3D geometric morphometric analysis (GMA).

Materials and Methods

The present analysis was conducted on a sample of 104 (M=50, F=54) post-mortem CT scans collected by the Department of Forensic Medicine, University of Copenhagen. These data contain adult individuals of documented sex. Individuals were scanned at a voltage peak of 120 kVp with slice thickness varying between 0.5mm and 2.0mm.

Segmentation and rendering of the data was done using Materialise MIMICS medical imaging software to create 3DCT models of the skull for each individual. From the 3DCT, 21 landmarks of the skull, as outlined in Moore-Jansen *et al.* (1994) (Table 1), were designated on each cranium in MIMICS (Figure 1). The coordinate data for each landmark and for each individual were then exported from MIMICS to PAST (PAleontological STatistics) software (Hammer *et al.* 2001) and SPSS statistical software programs for further analyses.

*Table 1. Alphabetized list of abbreviations for landmarks. *Left and right sides collected.*

Abbrev	Landmark Name
AL	Alare*
AU	Auriculare*
B	Bregma
BA	Basion
D	Dacryon*
EC	Ectoconchion*
EU	Euryon*
FMB	Foramen Magnum*
FMT	Frontomalare Temporale*
FT	Frontotemporale*
G	Glabella
GN	Gnathion
GO	Gonion*
ID	Infradentale
L	Lambda
N	Nasion
NS	Nasospinale
O	Opisthion
OP	Opisthocranion
PR	Prosthion
ZY	Zygion*

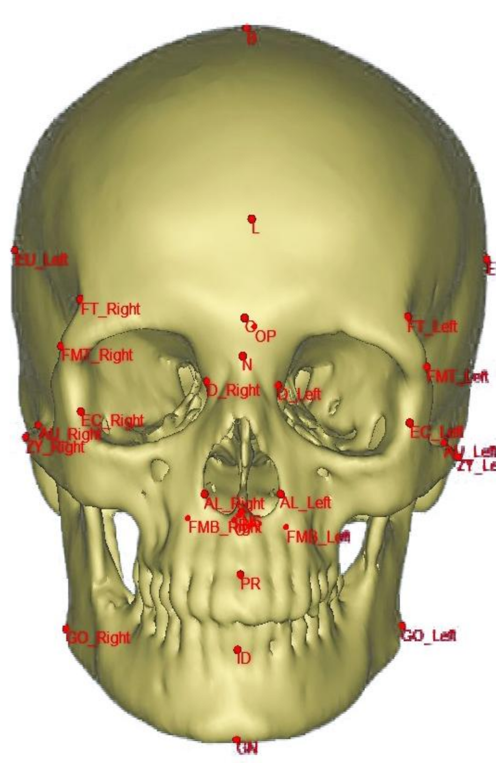

Figure 1. 3DCT skull model with landmarks designated.

Table 2. Alphabetized list of abbreviations for measurements and the landmarks used to generate the ILD between those measurements.

Abbrev	Measurement	Landmarks
AUB	Biauricular Breadth	AU-AU
BBHI	Basion Bregma Height	B-BA
BNL	Cranial Base Length	BA-N
BPL	Basion Prosthion Length	BA-PR
BGW	Bigonial Width	GO-GO
CH	Chin Height	GN-ID
DKB	Interorbital Breadth	D-D
EKB	Biorbital Breadth	EC-EC
FOB	Foramen Magnum Breadth	FMB-FMB
FOL	Foramen Magnum Length	BA-O
FRC	Frontal Chord	B-N
GOL	Maximum Cranial Length	G-OP
NLB	Nasal Breadth	AL-AL
NLH	Nasal Heigth	N-NS
OBB	Orbital Breadth (left)	D-EC
OCC	Occipital Chord	L-O
PAC	Parietal Chord	B-L
UFB	Upper Facial Breadth	FMT-FMT
UFH	Upper Facial Height	N-PR
WFB	Minimum Frontal Breadth	FT-FT
XCB	Maximum Cranial Breadth	EU-EU
ZYB	Bizygomatic Breadth	ZY-ZY

From the 3D coordinate data, inter-landmark distances (ILD) were used to generate 22 traditionally used 2D, linear craniometric measurements (Table 2). An independent samples t-test was used to test for significant differences between males and females in mean measurements. The ILD measurements of the skull predominantly capture size differences and to a lesser extent, shape differences. To investigate overall shape, independent of size, in the sample, GMA was conducted to analyze specific shape differences between the sexes. Generalized Procrustes Analysis was done to separate size and shape by rotating, scaling, and translating the raw coordinates of each cranium to the same relative position known as Procrustes Coordinates. Individuals with missing values were supported by column average substitution. Discriminant function analysis (DFA) was then performed using leave-one-out cross validation (LOOCV) and a forward Wilks' lambda stepwise selection on both the 2D and 3D data to determine how well the individuals within the sample correctly classified into the appropriate sex group. Finally, the DFA results were then visualized for the GMA using MorphoJ (Klingenberg 2011).

Results

Six ILDs were significantly different between males and females in this sample (Table 3; bold). Two variables (BGW & UFH) were included using stepwise selection of all 22 ILD in DFA. Using these two variables produced 74.0% cross-validated, combined classification accuracy with males classifying slightly better than females (Figure 2) (Table 4; ILD).

Table 3. Independent sample t-test for equality of means between males and females using ILDs.

ILD	t	df	Sig. (2-tailed)	Mean Difference
NLB	-2.756	102	0.007	-0.970780
AUB	-2.001	49.619	0.051	-15.61776
BBHI	-0.715	102	0.476	-22.90848
PAC	-1.090	102	0.278	-35.81912
FRC	-0.703	102	0.484	-21.51607
BNL	0.403	102	0.688	6.84743
FOL	0.794	102	0.429	7.793344
BPL	2.640	56.572	0.011	145.151930
DKB	-2.231	102	0.028	-0.988556
OBB	1.093	53.157	0.279	9.38420
EKB	0.777	53.185	0.441	10.788123
XCB	-2.713	102	0.008	-6.92574
FOB	0.547	102	0.586	13.94706
UFB	0.598	102	0.551	8.48085
GOL	0.524	102	0.602	7.29681
WFB	0.094	102	0.925	0.278979
CH	1.305	77.671	0.196	62.956376
BGW	-5.689	102	0.000	-7.112912
OCC	0.258	102	0.797	3.014750
NLH	0.737	102	0.463	11.276320
UFH	2.714	56.677	0.009	152.875602
ZYB	0.644	74.681	0.521	11.7961

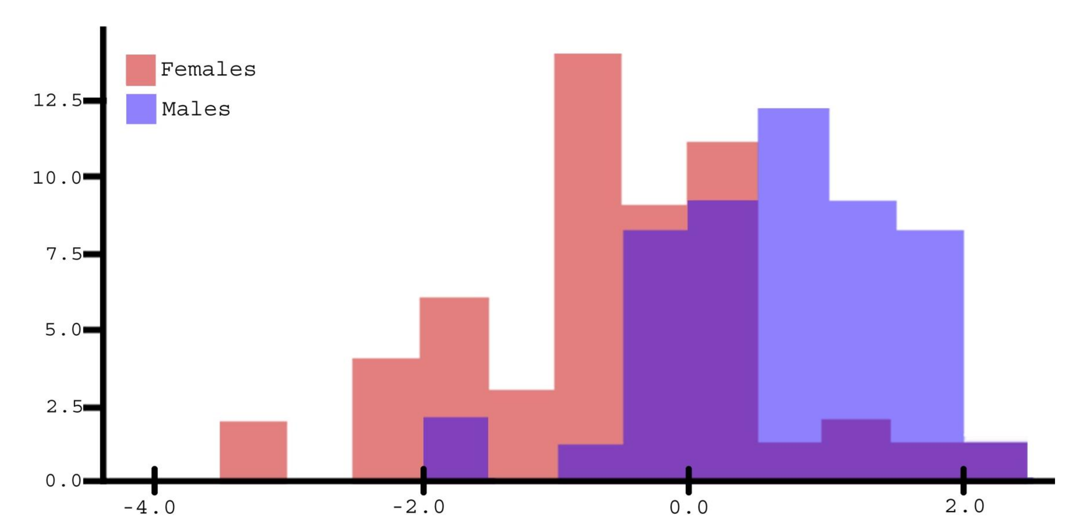

Figure 2. Two-way LOOCV DFA results for sex using two stepwise selected variables.

Table 4. LOOCV correct classification count for ILD and GMA using DFA with stepwise selection.

Data	Sex	Female	Male
ILD	Females	38	16
	Males	11	39
GMA	Females	38	16
	Males	14	36

The Procrustes Coordinates produced 71.2% cross-validated, combined classification accuracy with males again classifying slightly better than females (Table 4; GMA) (Figure 3). Five coordinates were selected in the stepwise analysis: FMBR_Y, FMBR_X, L_Z, EUR_Z, GOR_Y. Males had markedly larger shape differences than females in specific regions (in order of extent of differences): prosthion, bregma, infradentale, foramen magnum left, foramen magnum right, euryon left, euryon right, zygion left, and zygion right (Figures 4-6; females represented by red dots & males represented by blue lines).

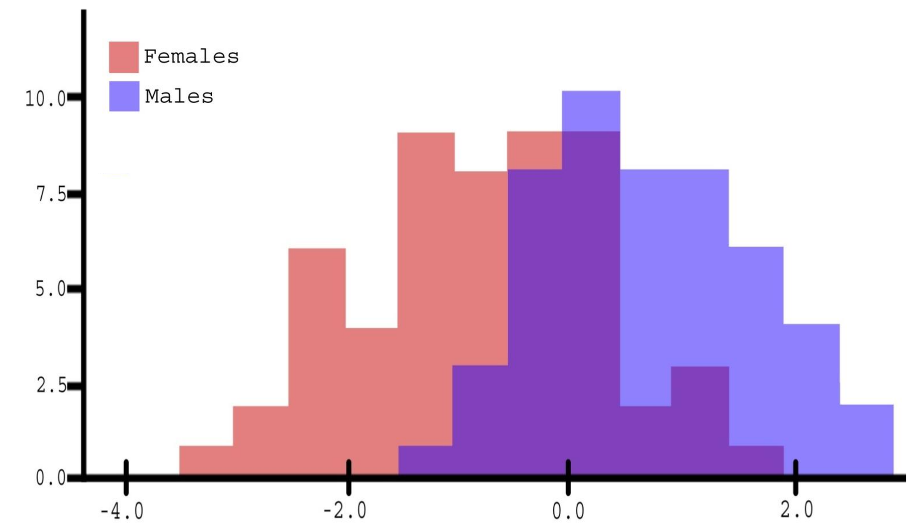

Figure 3. Two-way LOOCV DFA results for sex using five stepwise selected variables.

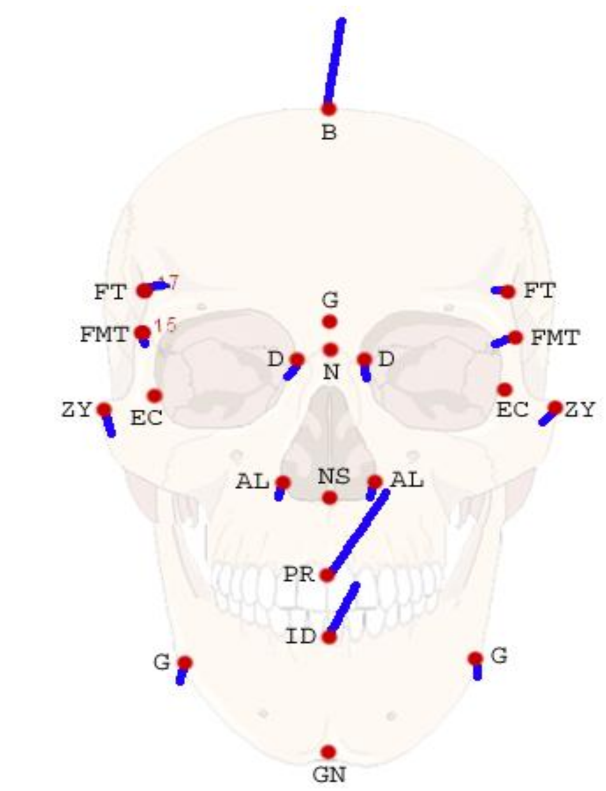

Figure 4. Mean landmark points for males and females after GMA in anterior view (photo from Wilkens & Williams 2001).

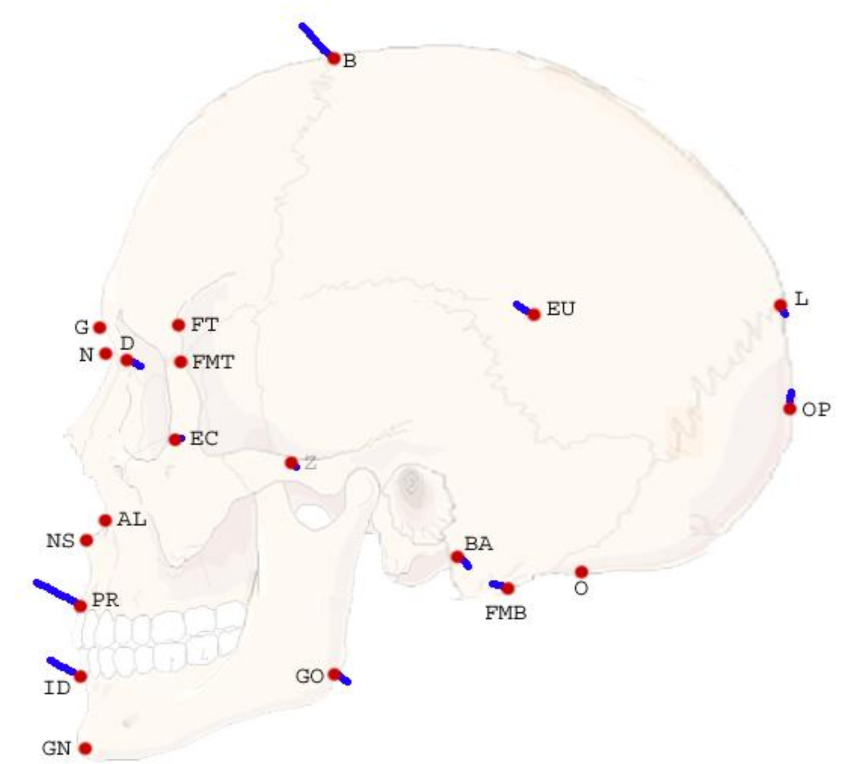

Figure 5. Mean landmark points for males and females after GMA in lateral view (photo from Wilkens & Williams 2001).

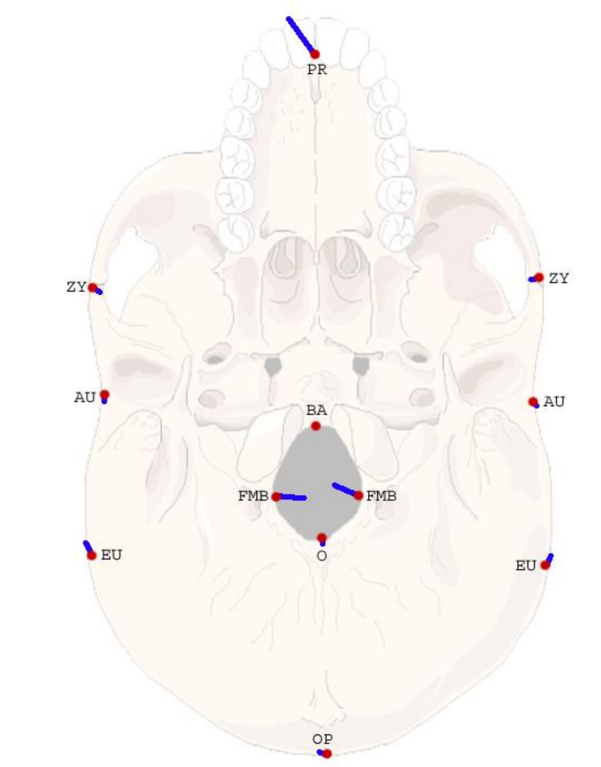

Figure 6. Mean landmark points for males and females after GMA in inferior view (photo from Wilkens & Williams 2001).

Discussion and Conclusions

Using traditional 2D measurements, bigonial width (GO-GO) and upper facial height (N-PR) best separated males and females based predominantly on size. Interestingly, these areas were not the areas of greatest differences between males and females in the shape analysis. Based on the greater displacement of the landmarks shown in Figures 4 to 6, males were generally more prognathic in the mouth region (PR & ID). They also tended to have larger shape differences in the width of the foramen magnum (FMB left & right) and in cranial breadth (EU left & right) than females.

References

Hammer Ø, Harper DA, Ryan PD. 2001. PAST: Paleontological Statistics Software Package for Education and Data Analysis. *Palaeontologia Electronica* 4:1-9.

Hildebolt CF, Vannier MW, Knapp, RH. 1990. Validation Study of Skull Three-Dimensional Computerized Tomography Measurements. *American Journal of Physical Anthropology* 82:283-294.

Kligenberg CP. 2011. MorphoJ: An Integrated Software Package for Geometric Morphometrics. *Molecular Ecology Resources* 11:353-357.

Moore-Jansen PH, SD Ousley, and RL Jantz. 1994. Data Collection Procedures for Forensic Skeletal Material (3rd ed.). Knoxville, Tennessee: University of Tennessee Forensic Anthropology Series.

Richtsmeier JT, Paik CH, Elfert PC, Cole III TM, Dahlman HR. 1995. Precision, Repeatability, and Validation of the Localization of Cranial Landmarks using Computed Tomography Scans. *Cleft-Palate Craniofacial Journal* 32:217-227.

Wilkens L, Williams B. 2001. Smart Draw LifeART collection images. Retrieved 17 October 2011 from <www.smartdraw.com>.

Williams FL, Richtsmeier JT. 2003. Comparison of Mandibular Landmarks from Computed Tomography and 3D Digitizer Data. *Clinical Anatomy* 16:494-500.

Acknowledgements

Canada Research Chairs / Chaires de recherche du Canada

This research was supported in part by the Canada Research Chairs program, University of Manitoba Graduate Fellowships and Manitoba Graduate Scholarships. Thanks also go to Michael Kenyhercz for editorial assistance.